Self- and Actin-Templated Assembly of Mammalian Septins

Makoto Kinoshita,[1] Christine M. Field,
Margaret L. Coughlin, Aaron F. Straight,
and Timothy J. Mitchison
Department of Cell Biology
Harvard Medical School
Boston, Massachusetts 02115

Summary

Septins are polymerizing GTPases required for cytokinesis and cortical organization. The principles by which they are targeted to, and assemble at, specific cell regions are unknown. We show that septins in mammalian cells switch between a linear organization along actin bundles and cytoplasmic rings, approximately 0.6 μm in diameter. A recombinant septin complex self-assembles into rings resembling those in cells. Linear organization along actin bundles was reconstituted by adding an adaptor protein, anillin. Perturbation of septin organization in cells by expression of a septin-interacting fragment of anillin or by septin depletion via siRNA causes loss of actin bundles. We conclude that septins alone self-assemble into rings, that adaptor proteins recruit septins to actin bundles, and that septins help organize these bundles.

Introduction

Septins are a family of conserved guanine nucleotide binding proteins involved in the remodeling of, or signaling from, the cell cortex. The biology of septins is poorly understood, but one clue comes from their localization in cells. In budding yeast, four septins, Cdc3p, Cdc10p, Cdc11p, Cdc12p, localize to the bud neck, where they play an important role in bud emergence and cytokinesis. In cultured mammalian cells, septins colocalize with actin structures, including actin bundles on the basal surface and arcs of F-actin at the perimeter (Kinoshita et al., 1997, Xie et al., 1999). We use the generic term "actin bundles" rather than "stress fibers," since the latter implies sarcomere-like organization (Cramer et al., 1997). Septins also localize to the cleavage furrow and are essential for cytokinesis in some systems (Neufeld and Rubin, 1994, Kinoshita et al., 1997). Septin-actin colocalization can be perturbed by drugs that disrupt actin organization (Kinoshita et al., 1997; Xie et al., 1999). However, neither the precise role of F-actin in septin organization nor the physiological significance of colocalization is understood. Progress in understanding spatial organization of septins will likely lead to insights into their molecular functions.

Septins occur in cytosol as heteromeric complexes of three to four different septin polypeptides that copurify with one molecule of tightly bound guanine nucleotide per septin polypeptide (Longtine et al., 1998; Field and Kellogg, 1999). Both heteromeric complexes (Field et

al., 1996) and an expressed single-septin polypeptide (Mendoza et al., 2002) tend to polymerize into filaments in vitro, although the role of GTP in the two reactions appears different (Mitchison and Field, 2002). The GTPase and polymerization activities of septins invite comparisons with tubulin and FtsZ, but this analogy might be deceiving; septins are more homologous to signaling GTPases than to tubulin, and their functions in yeast can be partially dissociated from their ability to polymerize (Frazier et al., 1998). Consistent with a cytoskeletal or membrane scaffold role, septins in the yeast bud neck have been shown to function in recruiting other components to the bud neck and to act as a diffusion barrier between mother and bud (Gladfelter et al., 2001). Septins have also been posited to play a role in membrane biology, perhaps regulating or targeting exocytosis (Hsu et al., 1998; Beites et al., 1999; Dent et al., 2002). These data hint at a role in coordinating exocytosis with actin activity, but the details are far from clear.

Progress on septin biochemistry has been slowed by the lack of pure complex for analysis of self-assembly and GTPase activities. Mammalian cells express multiple septin polypeptides, and defining the composition of septin complexes has been challenging (Hsu et al., 1998; Joberty et al., 2001; this study). In this study, we express a mammalian septin complex and test its ability to form discrete structures by both self- and actin-templated assembly in vitro. We also probe the role of septin-actin interaction in organizing both polymer systems in cells. In combination, these data reveal new principles for spatial organization of septins and reveal a role in actin organization in cells.

Results

Septin Organization in Cells Is Dynamic and Depends on Actin

To probe septin organization, we imaged two ubiquitously expressed mammalian septins, Sept2 (previously known as Nedd5; the new mammalian septin nomenclature will be used throughout this manuscript [Macara et al., 2002]) and Sept6 (previously known as Septin6), in mouse NIH3T3 fibroblasts. In interphase cells, these septins colocalized with actin in long linear bundles (Figures 1A and 1D), cortical arcs, and thicker bundles beneath nuclei (see below). When actin organization was disrupted with cytochalasin D, the majority of the Sept2 and GFP-Sept6 now localized in uniform rings (Figures 1B and 1E) with outer diameters of 0.66 ± 0.08 μm (mean ±SD, n = 111). Septins in cortical arcs were stable during cytochalasin treatment (Figure 1B). Sept2-containing structures fixed 5 min after the addition of cytochalasin (Figure 1C) and time-lapse observation of GFP-Sept6 (Figure 1D) suggested that the rings are formed by rolling up of linear septin bundles that dissociate from actin bundles on drug addition. Some of the rings formed during drug treatment tumbled about in the cytoplasm (Figure 1E), indicating that they are not

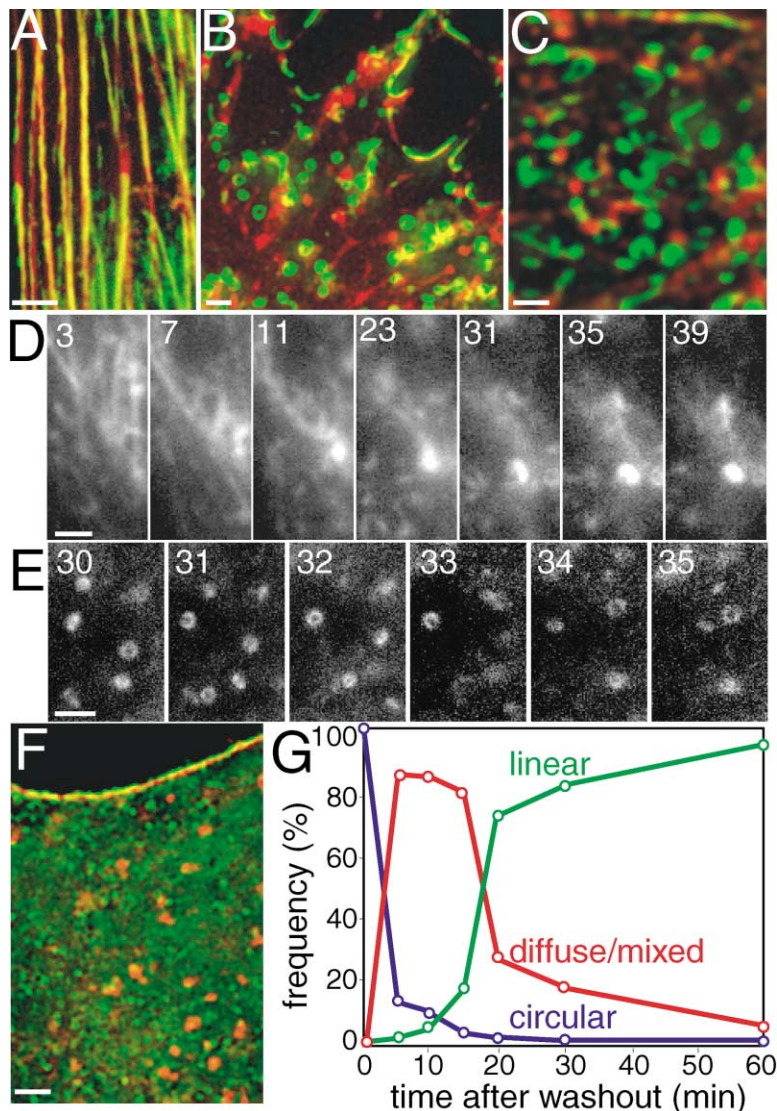[1]Correspondence: makoto_kinoshita@hms.harvard.edu

Figure 1. Effect of Cytochalasin D on Septin Organization

(A–C and F) Green, immunofluorescence staining of endogenous Sept2; red, phalloidin staining for F-actin. Scale bars, 1 μm in (A–F).
(A) Typical organization of septins along actin bundle in interphase NIH3T3 cells. Two other septins, Sept6 and Sept7, colocalized with Sept2 (data not shown).
(B) Cell treated with cytochalasin D for 30 min. Sept2 (as well as Sept6/7; data not shown) are now observed in rings, and not in linear bundles. In contrast, septin-positive arcs remain at the cell periphery.
(C) Cell treated with cytochalasin D for 5 min. A variety of transitional organizational states of septin structures are seen, from linear alignment along residual actin bundles to C- or O-shaped structures.
(D and E) Time-lapse images of GFP-Sept6-expressing cells after actin perturbation. The number in each frame denotes time (in minutes) after cytochalasin D addition.
(D) The linear septin structures roll up into rings.
(E) Some of the rings were tumbling around in the cytoplasm.
(F) A representative image of the cells 10 min after release from 30 min cytochalasin D treatment. Most of the septin rings have been replaced with diffuse or punctate signal. Note the relative stability of the cortical structure containing F-actin and septins.
(G) Time course after cytochalasin D washout after the 30 min treatment. Cells were classified into three categories by their septin structures: mostly rings, blue; diffuse, punctate, or mixture of rings and linear bundles, red; mostly linear bundles, green. The fraction of each category was plotted. n = 200 at each time point.

tightly associated with residual cytoskeleton or the plasma membrane. Similar rings were seen on jasplakinolide addition (data not shown) and in other cell types upon treatment with latrunculins (Xie et al., 1999).

Dissociation of septins from actin was reversible. Five minutes after cytochalasin washout, most of the rings disappeared, and septin localization was diffuse (Figure 1F). Twenty to thirty minutes after washout, coalignment of linear septin structures with actin bundles was restored (Figure 1G). These rapid changes in localization reveal that septin organization in interphase fibroblasts is dynamic and dependent on actin and suggest that the rings may represent a default assembly state, or storage form, of septins.

Expression of a Mammalian Septin Complex
To reconstitute septin assembly, we first needed to define a physiologically relevant complex. We affinity-purified septin complexes from mouse brains and HeLa cells with a peptide antibody to the ubiquitous septin, Sept2, eluting native complex with the cognate peptide (Figure

2A). The brain-derived septins had a complex polypeptide pattern, and HeLa cells had a simpler one. Immunoblotting and mass spectrometry of tryptic digests suggested that most of the polypeptides were septins in both cases. On the basis of these data, we chose Sept2, Sept6, and Sept7 (hCDC10) as ubiquitous septins that are likely to coassemble into a physiological complex. We coexpressed these polypeptides in insect cells by infection with multiple baculoviral vectors and purified them using a His$_6$ tag on Sept2, resulting in a complex with 1:1:1 stoichiometry of the three polypeptides (Figure 2A). Negative-stain EM revealed short filaments (range, 7–250 nm) with diameters of ~7 nm (Figure 2A). The gel filtration profile of the expressed complex was complicated, probably consisting of oligomers of the putative unit complex and a small amount of free Sept2, but the three septins exactly cofractionated in the higher-molecular weight range (Figure 2C), consistent with a 2:2:2 unit complex in *Drosophila* (Field et al., 1996). The complex contained tightly bound GDP:GTP at a ratio of 2.1:1 and a stoichiometry of ~1.2 nucleotides
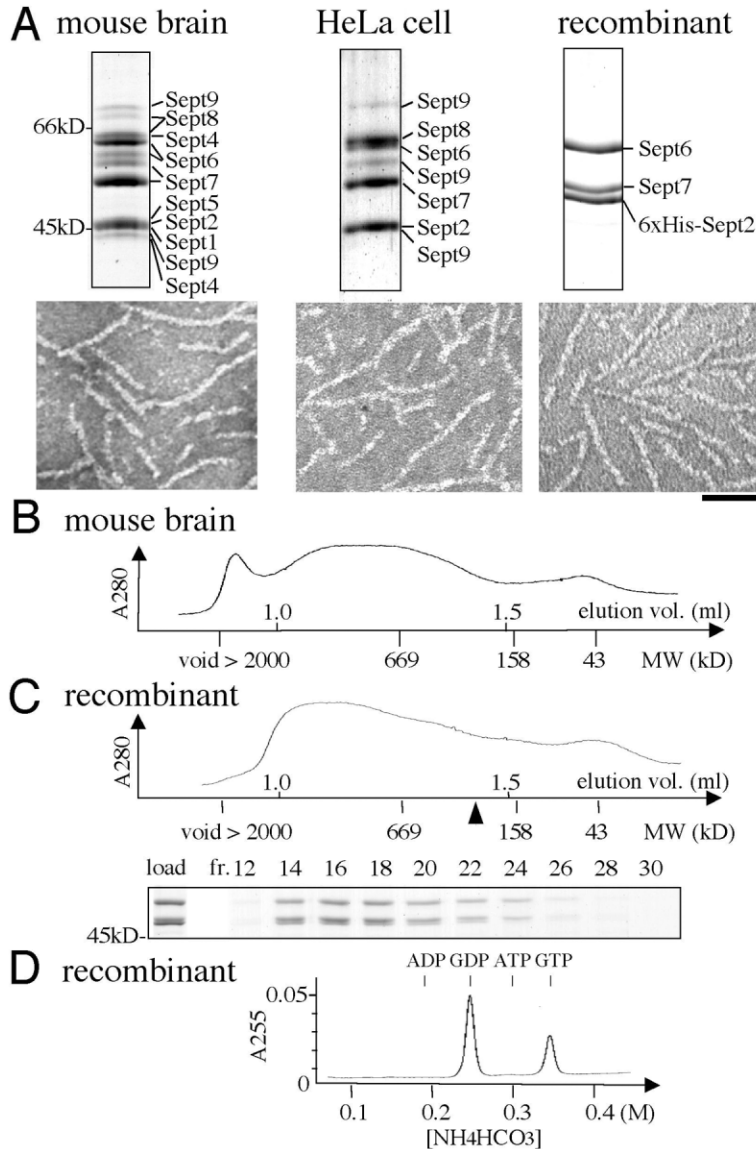
Figure 2. Comparison of Purified and Expressed Mammalian Septin Complexes

(A) SDS-PAGE analysis (Coomassie blue-stained) and negative-stain EM images of septin complexes purified from mouse brain, HeLa cells, and Sf9 cells coexpressing His_6-tagged Sept2, Sept6, and Sept7. Components identified by immunoblotting and mass spectrometry are denoted. The multiple sizes of the Sept4 and Sept9 bands are probably due to splice variants. By EM, each complex appeared as filaments of variable length. Bar, 100 nm.

(B) Gel filtration of brain-derived septin complex.

(C) Gel filtration of expressed complex. The arrowhead indicates the calculated size of putative 2:2:2 hexamer (286 kDa). SDS-PAGE/Coomassie staining showed near 1:1:1 stoichiometry of each fraction of the recombinant complex in all fractions.

(D) Guanine nucleotides released from denatured expressed complex separated by ion exchange chromatography. A representative trace showing that ~15 μg of the complex (~315 pmol septin polypeptides) contained 265 pmol of GDP and 126 pmol GTP, giving GDP:GTP ratios of 2.1 and ~1.2 guanine nucleotide per polypeptide.

per polypeptide (Figure 2D). Thus, our expressed complex resembles endogenous complexes from *Drosophila* (Field et al., 1996) and yeast (Frazier et al., 1998) by all criteria tested.

The Mammalian Septin Complex Self-Assembles into Rings

The expressed septin complex showed no change in structure by EM over 24 hr at 4°C in buffers containing 0.1–0.5 M KCl and 0.1 M imidazole. Dialysis into 0.05 M KCl without imidazole induced rapid lengthening and bundling of the filaments (Figures 3A, 3C, and 3D). Over 12–24 hr most of these bundles converted into uniformly curved coils and rings (Figures 3E–3H) in which Sept2, Sept6, and Sept7 were tightly colocalized (Figure 3I and data not shown). The outer diameter of these rings was 0.68 ± 0.09 μm by immunofluorescence (n = 45; Figures 3I and 3J) and 0.51 ± 0.07 μm by EM (n = 28), similar to the rings formed after cytochalasin treatments of cells. Self-assembly of expressed septin complex into

filaments, bundles, and rings was not measurably affected by the presence or absence of GTP, GDP, ATP, or nonhydrolyzable nucleotide analogs (data not shown). The ratio of bound GDP:GTP was virtually unchanged after dialysis for 24 hr (2.1:1 before versus 2.0:1 after), indicating that no hydrolysis of GTP occurred during assembly. We conclude that the pure septin complex has an inherent tendency to self-assemble into rings and that this accounts for the tendency of septins to form rings in cells when deprived of contact with actin bundles (Figures 1B–1E).

Anillin Can Mediate Septin Filament Organization along Actin Bundles

The expressed septin complex alone showed no detectable affinity for F-actin in cosedimentation and visual assays (Figures 4A and 5B), suggesting that an additional factor is required for recruitment of septins to actin bundles. Because of its ability to bundle F-actin (Field and Alberts, 1995) and its tight colocalization with
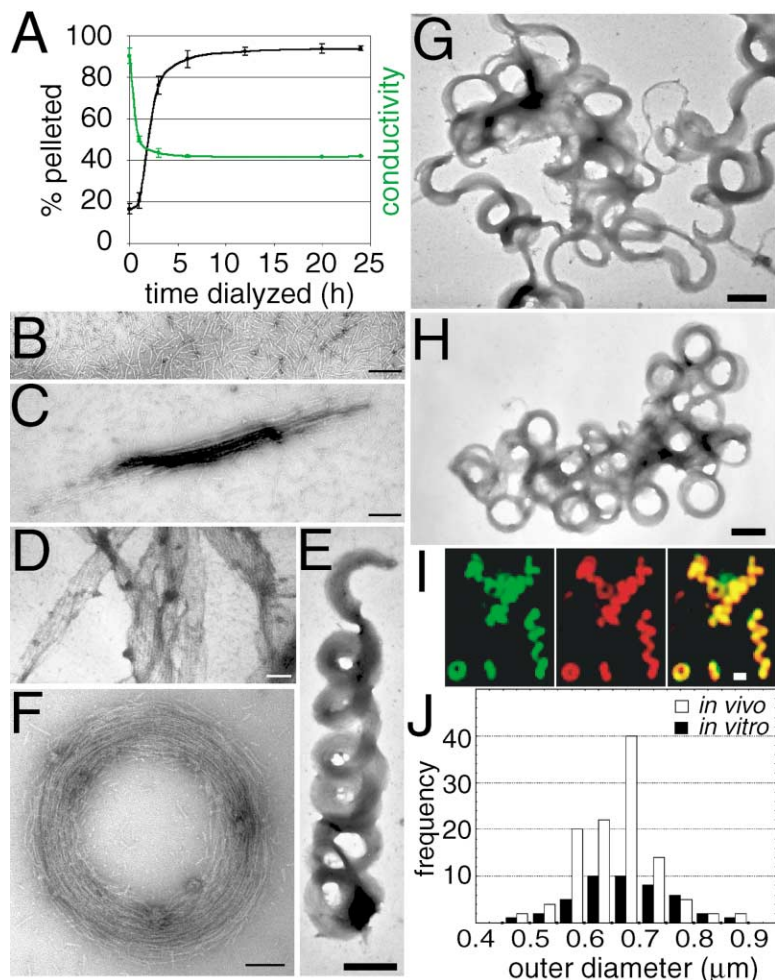
Figure 3. Self-Assembly of Expressed Septin Complex into Larger Structures

(A) Dialysis of purified, expressed septin complex into 50 mM KCl buffer promoted assembly of larger structures, as measured by sedimentation. The fraction of septins in the pellet and supernatant were measured by densitometry of SDS-PAGE/Coomassie-stained gels (black trace). Kinetics of dialysis were monitored by conductivity ($\times 0.7[[\Omega^{-1}m^{-1}]]$) (green trace). The error bars denote standard deviations of measurements performed in triplicate.

(B–H) Negative-stain EM images of expressed septin complex before and after dialysis. Thin bars, 100 nm; thick bars, 500 nm.

(B) Starting material (short filaments) in 0.1 M KCl plus 0.1 M imidazole.

(C and D) Three hours after dialysis. Ribbon-shaped bundles of longer filaments predominate.

(E–H) Twenty-four hours after dialysis. Spiral (E and G) and circular (F and H) bundles predominate.

(I) Immunofluorescence of spirals and rings after 24 hr dialysis stained for Sept2 (green) and Sept7 (red). Double staining for Sept2/6 gave similar results (data not shown). All three septins colocalized in the in vitro higher-order structures.

(J) Histograms of septin ring size distribution in cells after actin depolymerization (as in Figure 1B; open bars) and after 24 hr dialysis of expressed complex in vitro (closed bars). Outer diameter was measured in Sept2 immunofluorescence images.

septins in cells (Oegema et al., 2000), the contractile ring protein anillin is a candidate for such an adaptor. To test this, F-actin stabilized with phalloidin was incubated with several different actin-bundling/crosslinking proteins, allowed to adhere to a coverslip, incubated with the recombinant septin complex, fixed, and imaged by immunofluorescence. For biochemical experiments, we used *Xenopus laevis* anillin expressed in the baculovirus/Sf9 system. Fascin, filamin, anillin, and, to a lesser extent, α-actinin crosslinked the F-actin into large bundles (Figure 4). Only the anillin bundles efficiently recruited septin complex. We conclude that anillin is unique among the crosslinkers tested in that it can both organize actin filaments into bundles and recruit the septin complex.

To dissect the dual function of anillin, we expressed polypeptides truncated from the C terminus (Figure 5A) and used cosedimentation (Figure 5B) and imaging assays (Figure 5C) to assess their ability to bind F-actin and to mediate septin-actin interaction. Removal of a C-terminal region containing the PH domain and flanking conserved sequences generated a fragment (1–747) that could still bind and bundle actin but was not able to recruit septin complex, placing the septin-interacting region in the C-terminal third of anillin. A separate region nearer the N terminus was required for F-actin binding and bundling activity (Figures 5A and 5C). Partial cosedimentation of septins and anillin in the absence of actin

(Figure 5B, compare column 6 with columns 2 and 3) is consistent with interaction in the absence of F-actin, though quantitative assays will be required to critically address this issue.

Although anillin efficiently recruits septins to F-actin in vitro and may play this role in cells during cytokinesis, it is probably not responsible for recruiting septins to actin bundles in interphase cells. In most interphase NIH3T3 cells, we found, by immunofluorescence, that anillin was localized to the nucleus, as reported (Field and Alberts, 1995; Oegema et al., 2000). In a small population (<5%) of cells, anillin was mostly cytoplasmic. In these cells, a fraction of anillin was observed to colocalize with actin in cortical arcs and bundles, especially underneath the nucleus (data not shown). In these cells, septins and anillin tightly colocalized on the actin bundles. We hypothesize that another protein(s) that can interact with both actin and septin filaments plays the adaptor role in recruiting septins to interphase actin bundles, while anillin plays this adaptor role in the contractile ring during cytokinesis.

Septin Perturbation in Cells
Our reconstitution data predicted that expression of the C-terminal third of anillin in cells might have a dominant-negative effect on septin-actin interactions. To test this, we expressed human anillin residues 929–1125 (a fragment lacking the F-actin binding region) fused to GFP
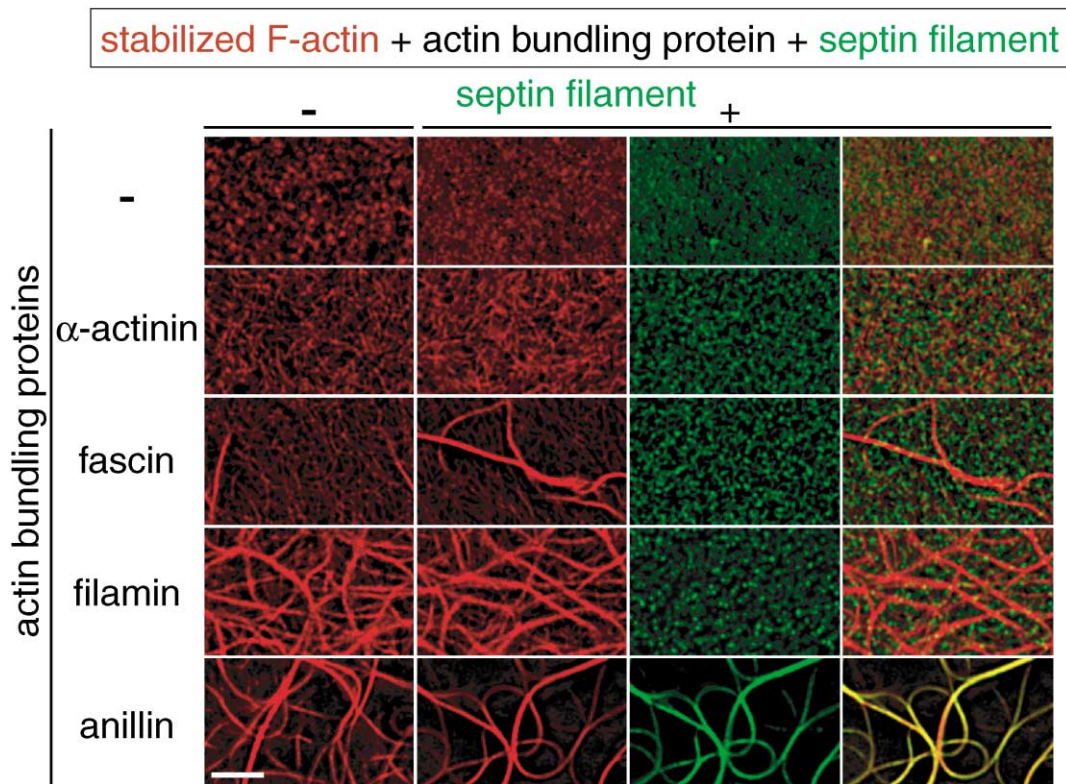
Figure 4. Anillin Bundles Actin and Recruits Septins

Visual assay for F-actin bundling and septin recruitment. F-actin stabilized with fluorescent phalloidin (red) was incubated with the bundling protein indicated, adsorbed to coverslips, incubated with expressed septin complex, fixed, and stained for Sept2 by immunofluorescence (green). All four bundling proteins caused some degree of filament bundling, and in no case did the addition of septins alter the appearance of bundles. Only anillin recruited septin complex to F-actin bundles. Bar, 5 μm.

in NIH3T3 cells. In cells expressing the fusion construct, septins were no longer localized to actin bundles on the basal surface, but, rather, they were localized diffusely in the cytoplasm, sometimes forming ectopic foci. Unexpectedly, the actin bundles themselves were attenuated or absent in ~80% of the expressing cells, with bundles under the nucleus particularly affected (Figures 6A–6C). In NIH3T3 cells, the fluorescence intensity in these subnuclear actin bundles tended to be brighter than elsewhere in cell (Figure 6B). In cells expressing GFP-anillin(929–1125), subnuclear actin bundles were strongly attenuated or missing, while more peripheral bundles and the F-actin associated with cortical arcs were less affected (Figures 6A and 6B). In cells expressing GFP alone, actin and septin staining were identical to the controls. These data support our biochemical conclusion that the C-terminal third of anillin interacts with septins. The loss of actin bundles was unexpected and suggests either that septin binding is required for actin bundle assembly/stability or that the anillin fragment has some additional, unpredicted effect on the actin cytoskeleton. To distinguish these possibilities we sought a different protein fragment that could sequester septins in cells. Borg3 is a human Cdc42 effector protein implicated in septin organization, and its BD3 domain (residues 83–110) is thought to interact directly with septins (Joberty et al., 2001). We expressed borg BD3 fused to GFP in NIH3T3 cells. The expressed fragment localized diffusely in the cytoplasm and often formed aggre-

gates. These aggregates strongly recruited septins, but not F-actin (Figure 6A). Actin bundles were disrupted by the BD3 fragment expression even more strongly than they were by anillin fragment expression (Figures 6A and 6B). Borg3(83–110) and anillin(929–1125) share no obvious sequence similarity and differ in isoelectric point (3.62 and 8.27, respectively). Since both fragments sequester septins and disrupt actin organization, we conclude that septins may be required for normal actin organization.

As a third method for testing the effect of septin removal on actin bundle organization, we used RNAi to deplete septins. NIH3T3 cells were transfected with a plasmid expressing hairpin siRNA designed to target either Sept2 or Sept7 transcripts. After 72 hr, Sept2 was reduced to 47% of the control by its cognate dsRNA, and Sept7 was reduced to 36% of the control level; immunoblotting was used to look at the whole-cell populations (Figure 7A). Sept2 levels were also slightly reduced by Sept7 knockdown and vice versa, suggesting that loss of one septin polypeptide may destablize another polypeptide from the same complex. Total protein expression, assayed by SDS-PAGE/Coomassie staining, was not affected (data not shown). Loss of a second septin when a first septin is ablated finds precedents in observations of lowered Sep1 level in pnut null *Drosophila* embryos (Fares et al., 1995) and of lowered Sept7 level in Sept5 (CDCrel-1) null mice (Peng et al., 2001). By immunofluorescence, septin staining was diminished
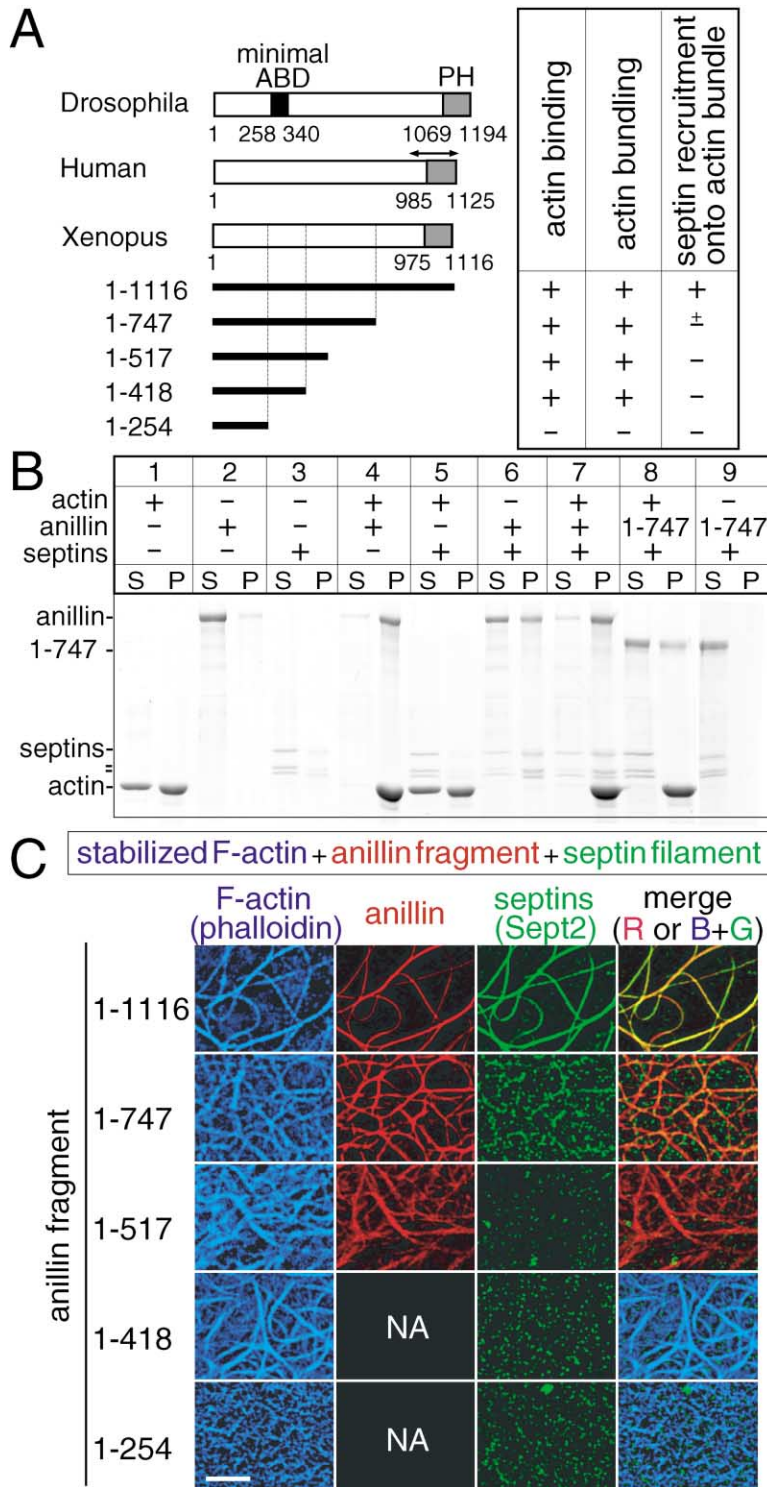
Figure 5. Mapping of Septin and F-Actin Binding Regions of Anillin

(A) Schematic comparison of *Drosophila*, human, and *Xenopus* anillins with serially truncated fragments of *Xenopus* anillin used in the study below. The minimal actin binding domain (ABD) was previously mapped for *Drosophila* anillin (Field and Alberts, 1995). PH, consensus for a plekstrin homology domain; a line with arrowheads represents the region of human anillin predicted to be required for septin binding by colocalization in cells (Oegema et al., 2000). A summary of the biochemical activities of the *Xenopus* anillin fragments is shown boxed on the right. Actin binding activity was scored by a cosedimentation assay without septins (data not shown). Actin-bundling activity was scored by visual assay without septins (C). Septin-recruiting activity was scored by cosedimentation (B) and visual assay (C).

(B) Cosedimentation of septin complex, F-actin, and anillin. Supernatants (S) and pellets (P) were analyzed by SDS-PAGE and Coomassie staining. Components were mixed as indicated and centrifuged at a speed chosen to pellet >75% of the F-actin (lane 1) while pelleting <25% of the anillin (lane 2) and <25% of the expressed septin complex (lane 3). Mixing anillin and F-actin caused >90% of both to pellet because of the formation of bundles (lane 4). Mixing septins with F-actin did not change the sedimentation of either (lane 5). Mixing septins and anillin caused a significant increase in the sedimentation of both, suggesting interaction and formation of larger assemblies, even in the absence of F-actin. Mixing all three components caused >75% of the septins to cosediment with the anillin/F-actin bundles (lane 7). An anillin fragment without PH domain did not promote cosedimentation with septins in either the presence (lane 8) or absence (lane 9) of F-actin.

(C) Visual assay for recruitment of septin complex to F-actin bundles by anillin fragments. Conditions were as in Figure 4, except that anillin fragments were used and that anillin was also immunostained. These data map the region of *Xenopus* anillin required to bundle F-actin to residues 255–418 and the region required to efficiently recruit septins to the bundles to residues 748–1116. The two shortest anillin fragments do not contain the epitope for the anti-anillin antibody (NA).

in 60%–70% of the transfected cells (Figure 7B). In cells where septin levels were obviously lowered by immunofluorescence, F-actin staining was perturbed. The thick actin bundles typically present under the nucleus of control cells were absent, and the remaining F-actin was restricted to the cell periphery (Figure 7B). In addition, septin-depleted cells were often wider and flatter than their neighbors. The phenotype was similar for both septins and different from those in other RNAi experiments in the laboratory (data not shown). Thus, the data from RNAi and dominant-negative expression agree, and we conclude that recruitment of septins is necessary to assemble or stabilize actin bundles in NIH3T3 cells, especially under the nucleus.
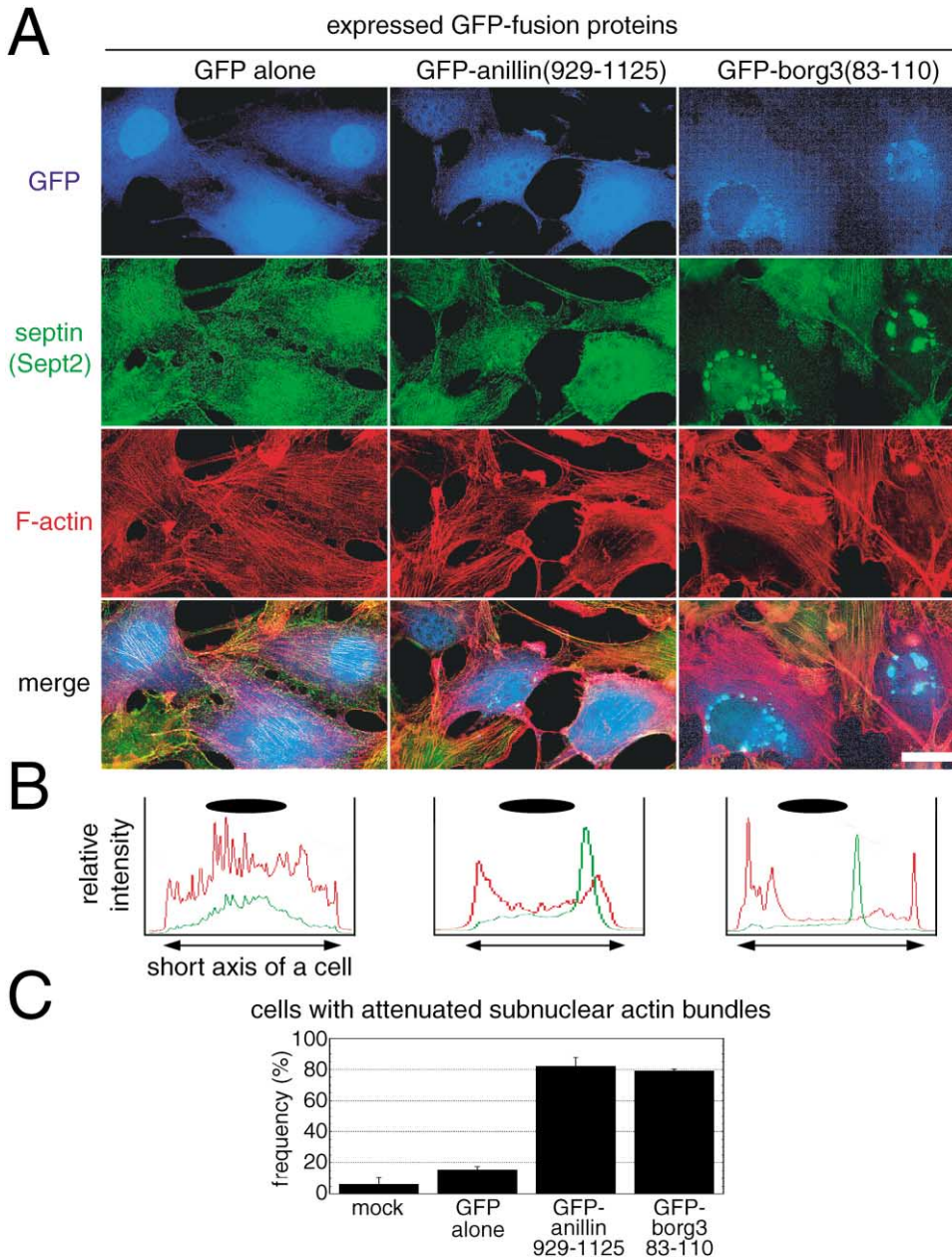
Figure 6. Septin Sequestration Attenuates Subnuclear Actin Bundles in NIH3T3 Cells

(A) Expression of septin-interacting regions of human anillin or borg3. Representative immunofluorescence images of endogenous Sept2 and F-actin in transfected NIH3T3 cells expressing GFP or GFP fusion proteins as labeled. Expression of each GFP fusion protein delocalized endogenous septins and occasionally sequestered them into cytoplasmic aggregates. Actin bundles, especially beneath the nuclei of these cells, are often attenuated or lost. Cells expressing GFP alone and the neighboring nontransfectants showed normal septin/actin status. Bar, 10 μm.

(B) Relative fluorescence intensities of Sept2 (green) and F-actin (red) measured along the short axis of the cell, across the center of the nucleus, in a representative transfected cell. The nuclear position (oval) and cell width (line with arrows) are shown for reference. Actin bundles and septins were abundant beneath the nuclei in cells expressing GFP alone and in neighboring mock-transfected cells (data not shown). In cells expressing GFP-human anillin(929–1125) or GFP-borg3(83–110), actin signals were markedly reduced under the nucleus but relatively unaffected at the cell periphery. The large peaks in the green channel indicate aggregates of endogenous Sept2.

(C) Quantitation of the effects on actin. Transfected cells with flat morphology were categorized by the status of subnuclear actin bundles, either normal or attenuated. Neighboring nontransfected cells on the same coverslips served as controls (mock). The percentage of affected cells (average ±SD) is plotted from three to four experiments, counting 50–70 cells in each experiment.

Discussion

Self-Assembly of Septin Complex into Rings

Our progress in setting up an in vitro system for analyzing the biochemistry underlying the spatial organization of septins is summarized in Figure 8. Our expressed complex resembles endogenous mammalian, *Drosophila*, and yeast complexes by all criteria tested and is suitable for probing spatial organization mechanisms. The expressed septin complex spontaneously self-
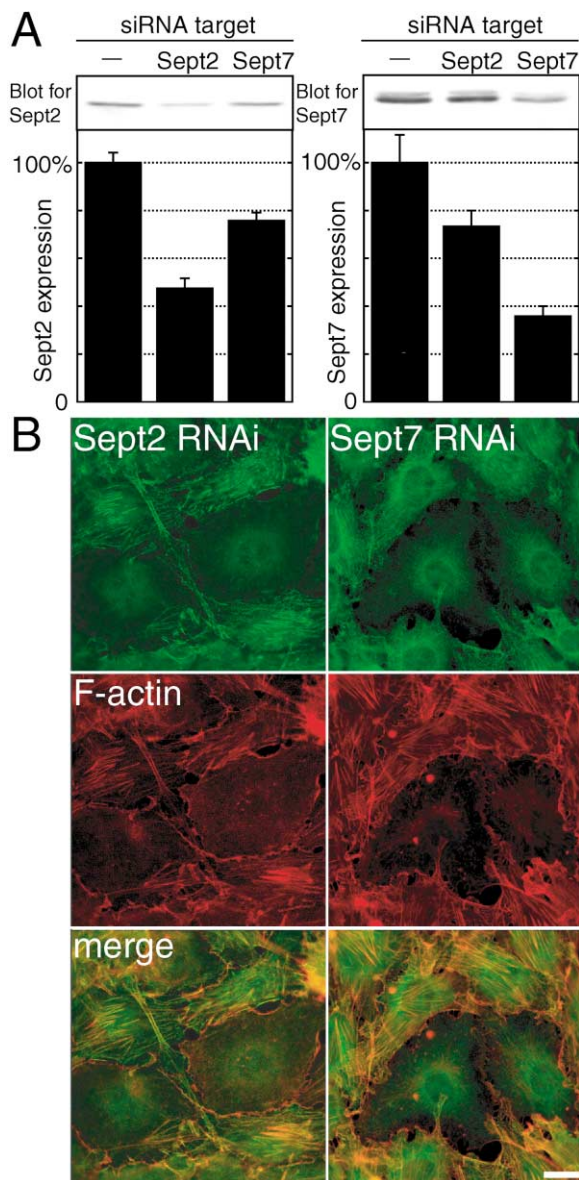
A

B

Figure 7. Depletion of Septins by RNAi Results in Attenuation of Actin Bundles

(A) NIH3T3 cells transfected with mU6pro vector expressing GFP or a unique sequence targeting either Sept2 or Sept7 were harvested after 72 hr and immunoblotted for the endogenous septins. The representative blots are shown at the top. The transfection efficiency monitored by mU6pro vector (which express GFP) was 60%–70%. The relative amounts of Sept2 and Sept7 proteins were quantified by densitometry, normalized to give 100% for the controls, and shown as graphs (average ±SD of triplicate experiment).
(B) Representative images of NIH3T3 cells 72 hr after transfection of plasmids that express hairpin siRNAs silencing either Sept2 or Sept7. The targeted septin was stained and shown in green. The two cells with diminished septin staining in the center of each image have few, if any, subnuclear actin bundles, though peripheral arcs still contain F-actin. After RNAi, >90% of the cells with diminished septin staining showed a similar phenotype, to a variable extent, and many were also wider or flatter than neighboring untransfected cells. Bar, 20 μm.

assembled into rings of uniform diameter that resemble rings formed in cells in the presence of an actin-perturbing drug. In the in vitro rings, individual septin filaments run circumferentially (Figure 3E), as if the structure is made from a bundle that curls up (Figure 8A). We expect a similar organization of rings in cells, since they appear to form by the curling up of linear arrays (Figures 1D and 8B). Given the similarity of the rings in vitro and in cells, we hypothesize that a basic tendency of septins to bundle and circularize drives ring formation in cells. That said, septin ring assembly is much faster in cells than in vitro, so some factors may promote ring assembly in cells. Likewise, rapid dissociation of septin rings after cytochalasin washout (Figures 1F and 1G) may be mediated by unknown cellular factors because septin rings appear very stable in vitro. The driving force for assembly of septins into rings of relatively constant diameter could have two origins. Individual septin polymers might have a defined curvature, or individual filaments might be flexible and the curved bundles could have a lower free energy than linear ones. In the cases of two other polymerizing GTPases, tubulin and FtsZ, individual protofilaments are straight in the GTP-bound form, but curved in the GDP-bound form, and this difference leads to dynamic instability of tubulin and perhaps to ingression of FtsZ rings during bacterial cytokinesis (Erickson, 2001). Our current data do not support a nucleotide-regulated curvature of mammalian septin filaments. We see no influence of added nucleotide on self-assembly nor do we observe hydrolysis of the tightly bound nucleotide [see, however, Mendoza et al. (2002) for nucleotide-dependent polymerization of a single septin polypepetide]. Since the septin bundles formed in the first few hours of dialysis are not curved (Figures 3C and 3D), we suspect that mammalian septin filaments do not have inherent curvature. Septin filaments are flexible, and we hypothesize that they tend to roll up into rings of 0.5–0.7 μm diameter. Actin filaments, flexible polymers with no inherent curvature, have also been observed to form rings under certain conditions (Tang et al., 2001). Given the tendency of septins to assemble into rings both in vitro and in cells, it is natural to ask whether these rings have any function. The cytochalasin addition/washout experiment (Figure 1) suggests that rings represent a storage form, or default assembly state, that provides a cytoplasmic pool ready to be recruited to F-actin bundles by an adaptor. Another possibility, suggested by similar diameters, is that the rings we observe are related to the organizational state of septins in narrow necks of cytoplasm, where they assemble under the plasma membrane. Examples include the yeast bud neck (diameter, 0.42–0.54 μm; Byers and Goetsch, 1976), the intercellular bridge after cytokinesis (~0.5 μm; Mullins and Biesele, 1977), ring canals during *Drosophila* spermatogenesis (1–1.5 μm; Hime et al. 1996), and the stalks that connect *Drosophila* blastomeres to the yolk sac after cellularization (~0.5 μm; Robinson and Cooley, 1996). Septins are thought to help stabilize such narrow necks and to recruit other factors. Their inherent ring-forming ability might be important for assembly in these locations. However, the organizational state of septins in cytoplasmic necks is controversial. In the yeast bud neck, classic EM data suggested that septin filaments are organized cirumferentially, as

A Actin-independent septin assembly

unit complexes   filaments   linear bundles   coiled and circular bundles

B Actin-templated septin assembly

actin bundle   actin / adaptor / septin
+
adaptor proteins   bundle
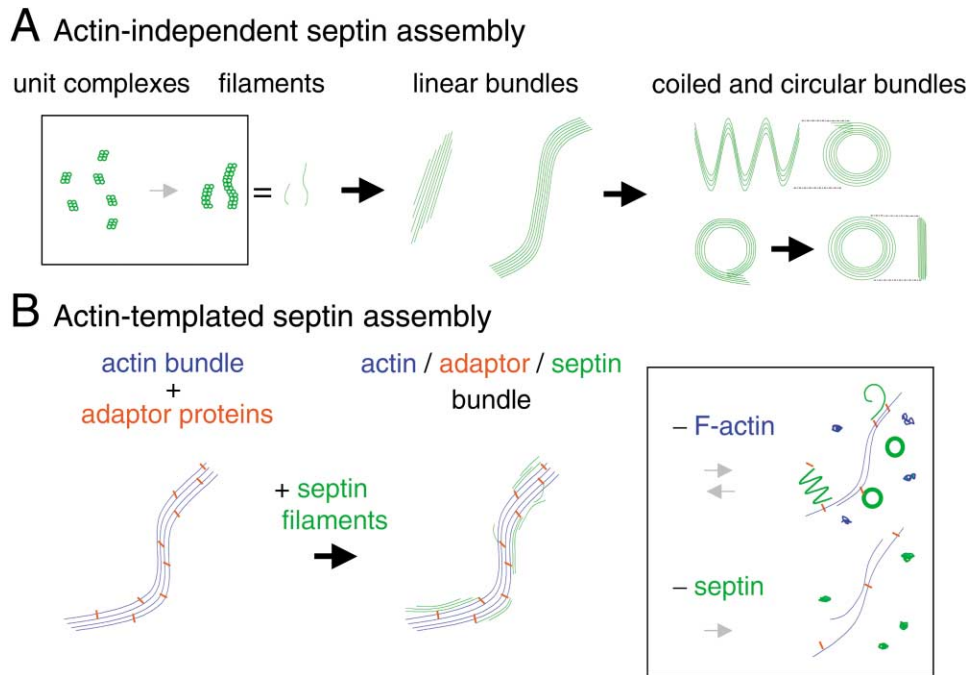
+ septin
filaments

− F-actin

− septin

Figure 8. Schematic Diagram of Self- and Actin-Templated Organization of Septin Complex

(A) Self-organization of septins. Higher-order organization processes reproduced in vitro with expressed mammalian septin filaments are shown with large arrows. This study has not addressed the process to generate putative unit complex and short filaments (denoted with small arrows), which occurs in eukaryotic cells (denoted as a box).

(B) Actin-templated organization of septins. An adaptor protein, such as anillin (red), organizes actin filaments (blue) into bundles while recruiting septin filaments (green) to the bundles. Anillin may be the major adaptor protein during cytokinesis, while an unidentified protein plays this role in interphase. When F-actin is disorganized by a drug (−F-actin), septins revert to the ring organization that predominated during self-assembly. When septins are removed by dominant-negative fragments or RNAi (−septin), F-actin bundles are destabilized.

in our rings (Byers and Goetsch, 1976). More recent data was interpreted as suggesting axial organization, different from our rings (Field et al., 1996; Longtine et al., 1998). Resolving the organizational state of septins in bud necks in cells will be necessary for progress on the biochemistry underlying this organization.

Actin-Templated Assembly of Septins

In interphase mammalian cells, most septins colocalize with actin bundles. Our biochemical data suggest that recruitment of septins to actin bundles is indirect, requiring an adaptor protein that can bind to both actin and septins (Figure 8B). We show that anillin can serve this adaptor role in vitro, and the physiological relevance of this interaction is supported by both cytological and genetic data. Cytologically, anillin is colocalized with septins in cytokinesis (Oegema et al., 2000). Expression of truncation constructs containing the C-terminal third of anillin generates foci that recruit septins (Oegema et al., 2000), and one such construct causes delocalization of septins (Figure 6). Genetically, we have characterized several point mutants in anillin that give rise to maternal effect mutations in *Drosophila* (Field et al., 1999). These mutations cause disruption of septin localization at the cellularization front in the *Drosophila* embryo, consistent with a septin-anillin interaction in the embryo. Thus, physiological relevance of the septin-anillin interaction is supported.

Since anillin is largely confined to the nucleus in interphase, we hypothesize that septins are recruited by an unknown adaptor protein to interphase actin bundles, with anillin serving this role during mitosis. From our domain analysis, proteins with homology to the C-terminal third of anillin are candidates for interacting with septins. Orthologs of anillin are recognizeable in several metazoan species, including *C. elegans*, but not in yeast. However, two yeast proteins, Bud4p (*S. cerevisiae*) and Int1p (*C. albicans*), have C-terminal PH domains, like anillin, and share a limited sequence homology with the C-terminal third of anillin. Experimental evidence supports their functional interaction with septins (Sanders and Herskowitz, 1996; Gale et al., 2001). *S. pombe* also contains a protein with a similar conserved sequence (accession number AL136521, SPAPYUG7.03c). Structure modeling might identify a septin-interacting domain shared by these proteins and anillin.

Although our work was primarily directed at questions of spatial organization, it is interesting to consider possible functions of the septins that localize to actin bundles. The loss of actin bundles we observe when septins are either sequestered by the interacting domains of anillin and borg3 or depleted by RNAi suggests that one function of septins is to promote assembly or to stabilize actin bundles (Figures 6 and 7). In other words, spatial organization of actin and septins is at least partly codependent in interphase NIH3T3 cells. Many other factors are known to regulate actin bundles in cells, including

actin binding proteins and the Rho/Rac/Cdc42 pathways, and determining how septins fit into this larger picture will be challenging. Actin bundles under the nucleus were especially sensitive to septin removal, while peripheral bundles and arcs were less affected (Figures 6 and 7). Actin bundles under the nucleus also recruit a subset of septins in some cells (Xie et al., 1999). Perhaps these subnuclear actin-septin bundles have some special function connected to the nucleus, such as detecting the state of cytoplasmic organization and communicating it to the nucleus, as has been proposed for yeast septins (Barral et al., 1999; Longtine et al., 2000). Overall our experiments have revealed some of the mechanisms by which septins become spatially organized, and we have established a biochemical system for dissecting this process in greater detail. However, the molecular functions of septins remain enigmatic. At a biochemical level, understanding the role of GTP binding and hydrolysis by septins is perhaps the highest priority. At a cellular level, we need to understand precisely how septins are involved in cytokinesis, exocytosis, and other processes involving the cell cortex. The tools and systems we have developed in this study should facilitate progress in both areas.

Experimental Procedures

Cell Culture, Drug Treatment, Fluorescence Microscopy, and Antibodies

NIH3T3 cells were grown on glass coverslips in Dulbecco's modified Eagle's medium supplemented with 10% fetal bovine serum. The cells were treated either with 3 μM cytochalasin D, 0.5 μM latrunculin A, or 1 μM jasplakinolide. Actin drugs were washed out 0.5 hr later and fixed at several time points. Immunofluorescence staining and time-lapse microscopy were performed as described (Kinoshita et al., 1997). Optical sectioning and deconvolution were performed with a DeltaVision system (Applied Precision). Transfection was performed with FuGene6 (Roche) 18–24 hr before live observation or fixation. Two rabbits were immunized with a synthetic oligopeptide corresponding to the amino-terminal 18 residues of Sept2 conjugated to bovine serum albumin (BSA), and the pooled sera were affinity purified on the same peptide. Immunoblot methods and characterization of most other anti-septin antibodies were described (Kinoshita et al., 2000). Antibodies for Sept8/9/10 will be described elsewhere.

Immunoaffinity Purification, Size Fractionation, and Negative-Stain EM of the Septin Complex

Endogenous septin complexes were purifed by immunoaffinity as described (Oegema et al., 1998). In brief, the anti-Sept2 antibody (1 mg) was bound to ProteinA beads in IP buffer (20 mM Tris-HCl [pH8.0], 75 mM KCl, 0.5 mM EDTA, and 0.5 mM EGTA) for 1 hr and washed with the buffer. Mouse tissues and HeLa-S3 cells were homogenized in lysis buffer (20 mM Tris-HCl [pH8.0], 0.1 M KCl, 0.1% NP40, 0.5 mM EDTA, 0.5 mM EGTA, 1 mM dithiothreitol (DTT), 1 mM PMSF, and protease inhibitors). After centrifugation at 27,000 $\times$ g for 15 min, the supernatant was ultracentrifuged at 100,000 $\times$ g for 1 hr. The high-speed supernatant (HSS) was incubated with the affinity column for 4 hr. After washing the column extensively with IP buffer and high-salt buffers (20 mM Tris-HCl [pH8.0], 0.5–1 M KCl, 0.5 mM EGTA, 1 mM DTT, and 1 mM PMSF), the septin complex was eluted with the cognate peptide in the high-salt buffer. For gel filtration, the isolated complex was passed through a 0.45 μm filter and fractionated with a Superose 6 gel filtration column equilibrated with 20 mM Hepes [pH 7.4], 75 mM KCl, 10% glycerol, and 1 mM DTT. For negative stain EM, samples were adsorbed to glow-discharged, formvar-coated copper grid and stained with 1% uranyl formate. Each procedure was done at 4°C.

Expression and Purification of the Recombinant Septins and Anillin

A mouse cDNA fragment encoding Sept2/Nedd5 (99% identical to human Sept2; Kinoshita et al., 1997) was cloned into a plasmid vector, pFastbac-HTa (Invitrogen). Two human cDNA fragments, Sept6/KIAA0128 (95% identical to mouse Sept6; a gift from Dr. T. Nagase) and Sept7/hCDC10 (99% identical to mouse Sept7; a gift from Drs. S. Nakatsuru and Y. Nakamura; Nakatsuru et al., 1994), were cloned into pFastbac-Dual. While Sept7 was insoluble unless coexpressed with Sept6, His$_6$-tagged Sept2 and His$_6$-tagged Sept2/Sept6 were soluble (data not shown). Hence, we controlled the relative expression level of the three components as Sept7 $\geq$ Sept6 > His$_6$-tagged Sept2 to minimize potential contamination of the partial complexes. Sf9 cells coinfected with the baculovirus vectors for 48 hr were lysed in a buffer (20 mM potassium phosphate butter [pH 7.2], 0.5 M KCl, 1% NP40, 10% glycerol, 5 mM 2-mercaptoethanol, and protease inhibitors) and centrifuged at 100,000 $\times$ g for 1 hr. The HSS was incubated with Ni-NTA resin (Qiagen) for 1 hr. The resin-bound septin complex was washed with buffers (20 mM potassium phosphate butter [pH 7.2 and 6.0], 0.1–0.5 M KCl, 0.01 M imidazole, 10% glycerol, 5 mM 2-mercaptoethanol, and 1 mM PMSF) and eluted with a buffer (20 mM potassium phosphate butter [pH 7.2], 0.1–0.5 M KCl, 0.1 M imidazole, 10% glycerol, and 1 mM DTT). Each purification step was done at 4°C. Recombinant *Xenopus laevis* anillin (accession number AY180201) and the fragments were produced by similar methods, to be described in detail elsewhere (A.F.S., in preparation).

Self-Assembly of the Recombinant Septin Filaments

The recombinant filamentous septin complex was clarified by centrifugation at 100,000 $\times$ g for 1 hr. The supernatant was diluted to 0.1 mg/ml ($\sim$0.35 μM as hexamer) and dialyzed up to 48 hr against a buffer (5 mM potassium phosphate butter [pH 7.2], 0.05 M KCl, 10% glycerol, 2 mM MgCl2, and 1 mM DTT) with or without 0.5 mM GTP, GDP, ATP, 0.1 mM GTPγS, or 10 mM EDTA. The time course of the higher-order assembly was quantified by triplicated sedimentation at 100,000 $\times$ g for 10 min, and then SDS-PAGE, Coomassie staining, and densitometry were performed. Each process was performed at 4°C. The kinetics of dialysis were monitored with a conductivity meter. The septin structures at 3 hr, 6 hr, 12 hr, and 24 hr were observed by negative-stain EM or transferred to the glass surface, fixed with 3.7% formaldehyde in PBS for 10 min, blocked with 2% BSA and 0.01% Tween 20 in PBS for 0.5 hr, and visualized by immunofluorescence and deconvolution as described above. Similar results were observed without KCl in the dialysis buffer.

Visual Assay for Higher-Order Structures

Rabbit skeletal muscle G-actin (2 μM; Pardee and Spudich, 1982) was polymerized and stabilized in Buffer A (2 mM potassium phosphate butter [pH 7.2], 0.05–0.1M KCl, 10% glycerol, 2 mM MgCl2, 0.5 mM ATP, 2 mM EGTA, 0.1 mM DTT, and 2 μM unlabeled phalloidin) for 20 min. F-actin was mixed with 1 μM actin bundling protein, either bovine fascin, human filamin (Nakamura et al., 2002), rabbit α-actinin (Cytoskeleton), or *Xenopus* anillin (see above), and immediately applied to a poly-D-lysine-coated glass coverslips. After incubation for 20 min, 0.3 μM recombinant septin complex was added to each reaction, and incubation was performed for a further 20 min. The septin complex was either freshly purified and added directly into imidazole-containing elution buffer or stored, frozen, in the same buffer. Each incubation was done in a 25°C humid chamber. After removing the excess reaction mixture, structures on the glass surface were fixed, immunostained, and imaged as above.

Cosedimentation Assay

Mixtures of 3.7 μM F-actin with or without 2 μM anillin and 0.3 μM preclarified septin complex in Buffer A (containing 0.05–0.075 M KCl) were incubated at 25°C for 20 min and then sedimented at 70,000 $\times$ g at 22°C for 10 min. The supernatant and pellet were separately analyzed by SDS-PAGE/Coomassie staining.

Silencing Cellular Septins by Hairpin siRNA Expression

Several unique target sequences for the mouse *Sept2* and *Sept7* genes were cloned into mU6pro plasmid vector (Yu et al., 2002) for

hairpin siRNA expression. Two such constructs targeting GAAUAU UGUGCCUGUCAUUG in the *Sept2* transcripts and AGAAAGCUAG CAGCAGUGAC in the *Sept7* transcripts showed the highest silencing efficiency in NIH3T3 cells at 72 hr after transfection and were used throughout this study. Transfection was done with LipofectAM-INE Plus (Invitrogen) 72 hr before harvest for immunoblot or fixation for immunofluorescence. Transfection efficiency, monitored separately by GFP-expressing mU6pro plasmid, was 60%–70%.

References

Barral, Y., Parra, M., Bidlingmaier, S., and Snyder, M. (1999). Nim1-related kinases coordinate cell cycle progression with the organization of the peripheral cytoskeleton in yeast. Genes Dev. *13*, 176–187.

Beites, C.L., Xie, H., Bowser, R., and Trimble, W.S. (1999). The septin CDCrel-1 binds syntaxin and inhibits exocytosis. Nat. Neurosci. *2*, 434–439.

Byers, B., and Goetsch, L. (1976). A highly ordered ring of membrane-associated filaments in budding yeast. J. Cell Biol. *69*, 717–721.

Cramer, L.P., Siebert, M., and Mitchison, T.J. (1997). Identification of novel graded polarity actin filament bundles in locomoting heart fibroblasts: implications for the generation of motile force. J. Cell Biol. *136*, 1287–1305.

Dent, J., Kato, K., Peng, X.R., Martinez, C., Cattaneo, M., Poujol, C., Nurden, P., Nurden, A., Trimble, W.S., and Ware, J. (2002). A prototypic platelet septin and its participation in secretion. Proc. Natl. Acad. Sci. USA *99*, 3064–3069.

Erickson, H.P. (2001). FtsZ protofilament and attachment of ZipA: structural constraints on the FtsZ power stroke. Curr. Opin. Cell Biol. *13*, 55–60.

Fares, H., Peifer, M., and Pringle, J.R. (1995). Localization and possible functions of Drosophila septins. Mol. Biol. Cell *6*, 1843–1859.

Field, C.M., and Alberts, B.M. (1995). Anillin, a contractile ring protein that cycles from the nucleus to the cell cortex. J. Cell Biol. *131*, 165–178.

Field, C.M., Al-Awar, O., Rosenblatt, J., Wong, M.L., Alberts, B.M., and Mitchison, T.J. (1996). A purified *Drosophila* septin complex forms filaments and exhibits GTPase activity. J. Cell Biol. *133*, 605–616.

Field, C.M., and Kellogg, D. (1999). Septins, cytoskeletal polymers or signalling GTPases? Trends Cell Biol. *9*, 387–394.

Field, C.M., Doberstein, S., Brill, J., Yu, K., and Sullivan, W. (1999). The contractile ring anillin is essential for cell division-associated contractile events in the early Drosophila embryo. Mol. Biol. Cell. Suppl. *10*, 239a.

Frazier, J.A., Wong, M.L., Longtine, M.S., Pringle, J.R., Mann, M., Mitchison, T.J., and Field, C.M. (1998). Polymerization of purified yeast septins, evidence that organized filament arrays may not be required for septin function. J. Cell Biol. *143*, 737–749.

Gale, C., Gerami-Nejad, M., McClellan, M., Vandoninck, S., Longtine, M.S., and Berman, J. (2001). *Candida albicans* Int1p interacts with the septin ring in yeast and hyphal cells. Mol. Biol. Cell *12*, 3538–3549.

Gladfelter, A.S., Pringle, J.R., and Lew, D.J. (2001). The septin cortex at the yeast mother-bud neck. Curr. Opin. Microbiol. *4*, 681–689.

Hsu, S.C., Hazuka, C.D., Roth, R., Foletti, D.L., Heuser, J., and Scheller, R.H. (1998). Subunit composition, protein interactions, and structures of the mammalian brain sec6/8 complex and septin filaments. Neuron *20*, 1111–1122.

Hime, G.R., Brill, J.A., and Fuller, M.T. (1996). Assembly of ring canals in the male germ line from structural components of the contractile ring. J. Cell Sci. *109*, 2779–2788.

Joberty, G., Perlungher, R.R., Sheffield, P.J., Kinoshita, M., Noda, M., Haystead, T., and Macara, I.G. (2001). Borg proteins control septin organization and are negatively regulated by Cdc42. Nat. Cell Biol. *3*, 861–866.

Kinoshita, A., Noda, M., and Kinoshita, M. (2000). Differential localization of septins in the mouse brain. J. Comp. Neurol. *428*, 223–239.

Kinoshita, M., Kumar, S., Mizoguchi, A., Ide, C., Kinoshita, A., Haraguchi, T., Hiraoka, Y., and Noda, M. (1997). Nedd5, a mammalian septin, is a novel cytoskeletal component interacting with actin-based structures. Genes Dev. *11*, 1535–1547.

Longtine, M.S., Fares, H., and Pringle, J.R. (1998). Role of the yeast Gin4p protein kinase in septin assembly and the relationship between septin assembly and septin function. J. Cell Biol. *143*, 719–736.

Longtine, M.S., Theesfeld, C.L., McMillan, J.N., Weaver, E., Pringle, J.R., and Lew, D.J. (2000). Septin-dependent assembly of a cell cycle-regulatory module in Saccharomyces cerevisiae. Mol. Cell. Biol. *20*, 4049–4061.

Macara, I.G., Baldarelli, R., Field, C.M., Glotzer, M., Hayash, Y., Hsu, S.-C., Kennedy, M.B., Kinoshita, M., Longtine, M., Low, C., et al. (2002). Mammalian septins nomenclature. Mol. Biol. Cell *13*, in press.

Mitchison, T.J., and Field, C.M. (2002). What does GTP do for septins? Curr. Biol., in press.

Mendoza, M., Hyman, A.A., and Glotzer, M. (2002). GTP-binding induces filament assembly of a recombinant septin. Curr. Biol. *12*, 1858–1863.

Mullins, J.M., and Biesele, J.J. (1977). Terminal phase of cytokinesis in D-98s cells. J. Cell Biol. *73*, 672–684.

Nakamura, F., Osborn, E., Janmey, P.A., and Stossel, T.P. (2002). Comparison of filamin A-induced cross-linking and Arp2/3 complex-mediated branching on the mechanics of actin filaments. J. Biol. Chem. *277*, 9148–9154.

Nakatsuru, S., Sudo, K., and Nakamura, Y. (1994). Molecular cloning of a novel human cDNA homologous to *CDC10* in *Saccharomyces cerevisiae*. Biochem. Biophys. Res. Commun. *202*, 82–87.

Neufeld, T.P., and Rubin, G.M. (1994). The *Drosophila peanut* gene is required for cytokinesis and encodes a protein similar to yeast putative bud neck filament proteins. Cell *77*, 371–379.

Oegema, K., Desai, A., Wong, M.L., Mitchison, T.J., and Field, C.M. (1998). Purification and assay of a septin complex from Drosophila embryos. Methods Enzymol. *298*, 279–295.

Oegema, K., Savoian, M.S., Mitchison, T.J., and Field, C.M. (2000). Functional analysis of a human homologue of the Drosophila actin binding protein anillin suggests a role in cytokinesis. J. Cell Biol. *150*, 539–552.

Pardee, J.D., and Spudich, J.A. (1982). Purification of muscle actin. Methods Enzymol. *85*, 164–181.

Peng, X.R., Jia, Z., Zhang, Y., Ware, J., and Trimble, W.S. (2001). The septin CDCrel-1 is dispensable for normal development and neurotransmitter release. Mol. Cell. Biol. *22*, 378–387.

Robinson, D.N., and Cooley, L. (1996). Stable intercellular bridges in development: the cytoskeleton lining the tunnel. Trends Cell Biol. *6*, 474–479.

Sanders, S.L., and Herskowitz, I. (1996). The BUD4 protein of yeast, required for axial budding, is localized to the mother/BUD neck in a cell cycle-dependent manner. J. Cell Biol. *134*, 413–427.

Tang, J.X., Kas, J.A., Shah, J.V., and Janmey, P.A. (2001). Counter-ion-induced actin ring formation. Eur. Biophys. J. *30*, 477–484.

Xie, H., Surka, M., Howard, J., and Trimble, W.S. (1999). Characterization of the mammalian septin H5: distinct patterns of cytoskeletal and membrane association from other septin proteins. Cell Motil. Cytoskeleton *43*, 52–62.

Yu, J.Y., DeRuiter, S.L., and Turner, D.L. (2002). RNA interference by expression of short-interfering RNAs and hairpin RNAs in mammalian cells. Proc. Natl. Acad. Sci. USA *99*, 6047–6052.

Accession Numbers

The GenBank accession number for *Xenopus laevis* anillin is AY180201.